Study of the variability of the Mediterranean Outflow Water using a Marginal Sea Boundary Condition in HYCOM

Alexandra Bozec[1], George R. Halliwell[2], Eric P. Chassignet[1], M. Susan Lozier[3]

1:Center for Ocean and Atmospheric Predictions Studies, Florida State University, Tallahassee, Florida
2: Rosenstiel School of Marine and Atmospheric Science, University of Miami, Miami, Florida
3: Earth and Ocean Sciences, Nicholas School of the Environment, Duke University, Durham, North Carolina

Submitted to Ocean Modelling

Corresponding Author:
Alexandra Bozec
COAPS Florida State University
227, RM Johnson Building
2035 E Paul Dirac Dr
Tallahassee, FL-32310
USA
Fax: 850-644-4841

Abstract:

Several questions remain unanswered about the role and importance of the Mediterranean Overflow Water (MOW) in the Atlantic Ocean. In this study, we investigate the variability of MOW and more specifically the extent to which MOW variability is driven by buoyancy forcing changes within the Mediterranean Sea and/or variability in the properties of the entrained waters. To answer this question, we use a 1/3° North Atlantic configuration of the HYbrid Coordinate Ocean Model (HYCOM). To allow for an accurate representation of the outflow properties, the Marginal Sea Boundary Condition developed by Price and Yang (1998) is implemented in HYCOM to parameterize the Mediterranean overflow. Sensitivity experiments in which T/S properties are fixed in the Atlantic and/or the Mediterranean are contrasted with a control experiment in which the overflow properties are free to adjust.

We found not only that MOW is more sensitive to variations of entrained water properties than source water properties, but also that the strength of the entrainment based on the density difference between the source and entrained water is critical to understanding the variability of this water mass. Indeed, the entrainment controls the salt (heat) flux either by affecting the properties and/or the total transport of MOW, thereby the entrainment can partially influence the distribution of Mediterranean salt(heat) in the Atlantic.

Keywords: Mediterranean outflow water variability; Outflow processes; Gulf of Cadiz; Boundary conditions

1. Introduction

The Mediterranean Overflow Water (hereafter MOW) is produced by the mixing of Mediterranean Sea Water (MSW) and North Atlantic Central Water (NACW) in the Gulf of Cadiz. This water mass has long been recognized as an important contributor to the heat and salt content of the North Atlantic (Zenk, 1975; Reid, 1979). Many past studies have focused on its pathway to the northeastern Atlantic and its contribution to preconditioning the Nordic and Labrador Sea deep water formation (Reid, 1979; Lozier et al., 1995; McCartney and Mauritzen, 2001; Lozier and Stewart, 2008). The variability of the MOW however has received less attention. A major unanswered question is: how and to what extent does the climatic variability of the MOW influence the property changes and circulation of the Atlantic Ocean? As a first step to answer this question, we focus in this study on the source of variability of the MOW.

The analysis of observations collected over the latter half of the 20th century shows a significant positive trend in water mass characteristics of the MOW in the North Atlantic (Levitus et al., 2000; Arbic and Owens, 2001; Curry et al., 2003). In the vicinity of the Gulf of Cadiz, Potter and Lozier (2004) found a positive trend of 0.101 ± 0.024ºC/decade for temperature and 0.0283 ± 0.0067 psu/decade for salinity, suggesting that the MOW is changing more rapidly than the other water masses of the Atlantic Ocean. More recently, Leadbetter et al. (2007) compared the data from a 36ºN transect occupied in 1959, 1981 and 2005, and found a 20-year reversal of the MOW properties between 10º and 20ºW. They describe a warming and salinification between 1959 and 1981 and a cooling and freshening between 2005 and 1981. However, data collected in

the Mediterranean Sea suggest that both temperature and salinity of the Mediterranean Water at Gibraltar have been increasing over this time period but at a rate one third as large as the MOW trend (Rixen et al., 2005; Millot et al., 2006). Another possible source of MOW variability is the NACW entrained in the Gulf Of Cadiz. According to the results of Arbic and Owens (2001), NACW water properties below 500m at 36ºN in the eastern Atlantic displayed changes similar to MOW water properties between 1959 and 1981. The complementary study by Leadbetter et al. (2007) shows similar changes in both water masses from 1981 to 2005. The question is then: what is driving the variability of the MOW in the Atlantic? One method for answering this question is to use numerical models.

MOW variability has not been extensively explored in ocean model studies, primarily because the physical processes involved in outflows require very high spatial resolution and accurate representation of mixing processes. While the parameterization of outflows in z-coordinates (spurious numerical mixing) and terrain-following coordinates (pressure gradient errors) remain a challenge, dense overflows are naturally represented in isopycnal coordinates (Griffies et al., 2000). This coordinate system prevents spurious numerical diapycnal mixing with ambient water, enabling the flow to maintain its density as it descends along the slope. Instead, diapycnal mixing can be finely controlled by the chosen turbulence closure. Several parameterizations of entrainment based on the Richardson number exist, such as the K-Profile Parameterization (hereafter KPP, Large et al., 1994), the bulk entrainment parameterization (hereafter TP, Turner, 1986; Hallberg, 2000) and more recently an algebraic entrainment parameterization (hereafter TPX, Xu et al., 2006). While KPP induces mixing too weak for a proper representation of an

entrained gravity current (Chang et al., 2005), TP and TPX were able to correctly reproduce the observed entrainment such as the one occurring in the Mediterranean outflow process (Papadakis et al., 2003; Xu et al., 2007). However, such a scheme requires a fairly high horizontal resolution and an explicitly resolved Mediterranean Sea with a thermohaline circulation able to produce realistic dense water at the Gibraltar sill. The most commonly used method in climate models that does not require any conditions in terms of vertical or horizontal discretization is a relaxation to climatological T and S in the Gulf of Cadiz. However, in this case, the properties of the outflow waters vary only seasonally, making this parameterization unsuitable for the study of interannual and decadal variability. Here, an intermediate approach is considered: the Marginal Sea Boundary Condition of Price and Yang (1998) (hereafter MSBC). As with the relaxation method, the entrainment processes do not need to be explicitly resolved with the MSBC, but the parameterization of the entrainment is based on TP. Moreover, as the MSBC uses water mass properties produced by the ocean model, the outflow water properties will vary on time scales produced by the ocean model.

The performance of the MSBC has been evaluated in a 1/12º HYbrid Coordinate Ocean Model (HYCOM) configuration of the Gulf of Cadiz region and very similar responses were found between the TPX and the MSBC when analyzing changes in the freshwater balance of the Mediterranean Sea (Xu et al., 2007). The MSBC has also been implemented by Wu et al. (2007) in the ocean component of the NCAR Community Climate System Model version 3 (CCSM3): the Parallel Ocean Program (Smith and Gent, 2004). Comparing the effect of a parameterized MOW on the thermohaline circulation using coupled and uncoupled experiments, Wu et al. (2007) show that the

Mediterranean tongue was correctly represented despite the low horizontal resolution (3º). We thus consider this parameterization suitable for our study.

The goal of this study is to 1) present the implementation of the MSBC in HYCOM, 2) present its application to a 1/3º resolution configuration of the Atlantic Ocean in order to study the sensitivity of the MOW to variations in the source water (Mediterranean Sea water, i.e. MSW) and entrained water (North Atlantic Central water, i.e. NACW) and finally 3) evaluate the consequences on the MOW properties in the Atlantic Ocean.

The paper is organized as follows: The ocean model and the implementation of MSBC is presented in section 2. A review of the water masses involved in the MOW processes is given in section 3. An evaluation of the sensitivity of MOW using the MSBC is presented in section 4, followed by a summary/discussion in section 5.

2. Presentation of the models

2.1 HYCOM

In this study, an Atlantic Ocean configuration of the HYbrid Coordinate Ocean Model (HYCOM) (Bleck, 2002; Chassignet et al., 2003; Halliwell, 2004) is used. The vertical discretization in HYCOM combines z coordinates at the surface, isopycnic coordinates in stratified open ocean and sigma coordinates over shallow coastal regions. The 1/3º resolution model domain extends from 90°W to 30°E and from 20°S to 70°N (Figure 1) and does not include the Mediterranean Sea. The bottom topography is derived from DBDB5 (National Geophysical Data Center, 1985). The vertical discretization uses 28 hybrid layers whose σ_2 target densities range from 23.50 to 37.48 kg/m^3. The initial

conditions in temperature and salinity are given by the General Digital Environmental Model (GDEM3; Teague et al. 1990). Relaxation to climatology is applied at the northern and southern boundaries in 10° buffer zones. The horizontal background viscosity is ~350 m^2s^{-1} and the deformation dependent viscosity coefficient is 0.2. Vertical mixing is provided by the KPP model (Large et al., 1994).

Climatological atmospheric forcing is derived from the 1979-1993 ECMWF climatology (ERA15). To account for synoptic atmospheric variability, 6-hourly wind stress anomalies corresponding to the neutral Niño period (September 1984-September 1985) are added to the monthly wind stresses; wind speed is obtained from the 6-hourly wind stresses. The heat and freshwater fluxes are calculated using bulk formulae during model simulations. The heat flux is derived from surface radiation, air temperature, specific humidity, wind speed, and model sea surface temperature (hereafter SST). The freshwater flux consists of an evaporation minus precipitation budget (E-P) plus a relaxation to observed surface salinity with a 30 day time scale. Evaporation is calculated from bulk formulae using wind speed, specific humidity and model SST. Precipitation is given by COADS.

2.2 The Mediterranean Sea Boundary Condition

The MSBC is designed to be used when HYCOM is run at a horizontal resolution too low to resolve the Strait of Gibraltar. HYCOM is then run without a Mediterranean Sea and the Gulf of Cadiz becomes a boundary zone where the MSBC determines the water properties, depth range, and transport of the overflow water entering the Atlantic basin. The MSBC combines two models: (1) the Bryden-Stommel-Kinder model (Bryden

and Kinder, 1991), which estimates properties of the deep outflow water entering the Atlantic basin through the Straits of Gibraltar, and (2) the Price-Baringer Marginal Sea Boundary Layer model (Price and Baringer, 1994), which then calculates properties of the final overflow (product) water by entraining Atlantic interior water into the Gibraltar overflow water.

Characteristics of the MSBC are illustrated schematically in Figure 2. Using information about the surface waters of the Atlantic in the Gulf of Cadiz and the heat and evaporation budget over the Mediterranean Sea, the model computes the properties (temperature, salinity and transport) of the Mediterranean Sea water at Gibraltar and of the Mediterranean Outflow Water at depth. Though a relatively simple model of the outflow process, results from the MSBC have been shown to be as accurate as the results from the parameterization of Xu et al. (2007) for the Mediterranean outflow region.

Inputs to the MSBC are either specified or provided by the model at grid points just west of the Gulf of Cadiz boundary zone. Specified inputs are the mass (E-P) flux and the net surface heat flux averaged over the Mediterranean Sea, which are set to 0.55m/y and -13W/m^2, respectively. These values were altered from the original values used by Baringer and Price (1994; 1997) of 0.7m/y and 0W/m^2. The inputs provided by the model are Gibraltar inflow temperature and salinity (T_{atl}, S_{atl}) averaged over the upper 140m just west of the Gulf of Cadiz boundary zone, and the temperature and salinity of the entrained NACW (T_{ent}, S_{ent}), set to the values at a depth of 625m just west of the Gulf of Cadiz. The NACW water depth was changed to 625m from the value of 400m recommended by Price and Yang (1998) in order to yield more realistic MOW properties. Since the mean mass and heat fluxes over the Mediterranean Sea are kept constant, all

MOW variability results from water mass changes in the Atlantic Ocean just west of the Gulf of Cadiz boundary zone. The MSBC outputs are highlighted in red in Figure 2. These include four transports: Tr_{atl}, Tr_{gib}, Tr_{ent}, and Tr_{out}, with the first two being equal and opposite to each other. They also include the temperature and salinity of the Gibraltar outflow (T_{gib}, S_{gib}) and the MOW (T_{out}, S_{out}). The corresponding densities are calculated using the model equation of state.

Implementation of the MSBC in HYCOM is not straightforward because the MOW, which has a temperature and salinity calculated by MSBC, must be accepted by interior isopycnic layers such that the target isopycnic density in each accepting layer is preserved. Additionally, it is important to keep the injected water salinity (S_{out}) and the average temperature of the injected water as close as possible to the value calculated by the MSBC. Technical details of the MSBC implementation are presented in the Appendix.

In brief, the Price-Baringer Marginal Sea Boundary Layer model calculates the entrainment parameter φ as follows: $\varphi = 1 - F_{geo}^{-2/3}$ where the geostrophic Froude number F_{geo} is $F_{geo} = \sqrt{g'}\,\dfrac{\alpha}{f\sqrt{h_{geo}}}$ and g', the buoyancy anomaly between the Gibraltar water and the entrained NACW is $g' = g(\rho_{gib} - \rho_{ent}) = g\Delta\rho_d$, α is the slope of the continental slope, and h_{geo}, the thickness of the outflow. h_{geo} depends on the geometry of the strait before the shelf break, the geostrophic velocity of the flow in this area and on the velocity of the flow at the strait deduced from the maximal exchange formulation (see Price and Baringer (1994) for more details). With this formulation, the entrainment of NACW increases as the density difference between the two water masses increases, with the

functionality shown in Figure 3. Once calculated, the entrainment parameter is used to calculate the properties of the outflow water (Tr_{out}, T_{out}, S_{out}):

$$Tr_{out} = Tr_{gib}\frac{1}{1-\varphi} \qquad (1)$$

$$T_{out} = T_{gib} - (T_{gib} - T_{ent})\varphi \qquad (2)$$

$$S_{out} = S_{gib} - (S_{gib} - S_{ent})\varphi \qquad (3)$$

The value of φ ranges between 0 and 1. If φ equals 0, no entrainment occurs, the salinity of MOW (S_{out}) equals the salinity of MSW (S_{gib}). If φ tends to 1, a large entrainment occurs, the salinity of MOW (S_{out}) tends to the salinity of NACW (S_{ent}). From a study of the upper and lower core of the Mediterranean Outflow Water, Rhein and Hinrichsen (1993) evaluated the proportion of pure Mediterranean water at 7º30'W to be 28-29% (corresponding to $\varphi \sim$ 0.72-0.73). Later, Baringer and Price (1997) deduced from observations between 7º and 7º30'W in the Gulf of Cadiz an entrainment parameter of ~0.7. This result means that the signature of the entrained water is by definition more important than the signature of the Mediterranean Sea in the variability of the Mediterranean outflow water properties.

In this study, 1) we test the sensitivity of the MOW variability to density compensated ($\Delta\rho_d$ constant) change in entrained water properties in HYCOM and 2) we evaluate the impact of a change in the density difference ($\Delta\rho_d$) between MSW (ρ_{gib}) and NACW (ρ_{ent}) on the MOW variability in the Atlantic Ocean.

3. Validation of the MSBC in HYCOM

3.1 Mediterranean Outflow Water in the observations

The Mediterranean Overflow Water results from the transformation of fresh and warm surface Atlantic waters into dense and salty Mediterranean water through air-sea interactions (see review by Pinardi and Masetti, 2000). This dense water mass (MSW) flows back across the Strait of Gibraltar at depth and cascades along the slope in the Gulf of Cadiz mixing with the ambient North Atlantic Central Water (NACW) until it reaches its buoyancy depth around 1100m (Iorga and Lozier, 1999; Candela, 2001). The MOW then flows into the open Atlantic. In the observations, the θ/S properties of the Mediterranean Sea at Gibraltar have been estimated at 13ºC and 38.4 psu respectively (Baringer and Price 1997; Hopkins, 1999). During its descent along the slope, MSW mixes with NACW whose temperature ranges between 11.4ºC and 12.5ºC and whose salinity ranges between 35.6psu and 35.7psu (Price and Baringer, 1994). Finally, the MOW reaches its buoyancy depth between 800 and 1200m and is divided in two main cores: an upper one (600-750m) and a lower one (down to 1200m) (Zenk and Armi, 1990; Bower et al. 1997, Iorga and Lozier, 1999). The θ/S properties of the upper core are 12.89ºC/36.43psu and 12.17ºC/36.65psu for the lower core in the Gulf of Cadiz (Baringer and Price, 1997). However, considering the vertical and horizontal resolution of our study along with the fact that the MSBC assumes that a single core of MOW is injected into the interior Atlantic, the MOW will be represented as a unique core introduced in the Atlantic around 8.5ºW. Following the climatological data of Lozier et al. (1995) and the θ/S plot of Mazé et al. (1997; see their Fig. 3), the temperature and salinity of the main core are approximately 11ºC and 36.2psu in the vicinity of Cape St Vincent.

A wide range of transport estimates (from 0.2 to 1.8Sv; 1Sv = $10^6 m^3/s$) at

Gibraltar exists in the literature (see Astraldi et al., 1999), mostly due to the multiple methods used to obtain these estimates. However, most estimates from direct measurement of the flow give a transport between 0.7Sv (Baringer and Price 1997) and 1.2Sv (Lacombe and Richez, 1982). The total transport of MOW in the Gulf of Cadiz has been evaluated at 3-4 times the value at the sill (Rhein and Hinrichsen, 1993; Baringer and Price 1997).

3.2 Mediterranean Outflow Water in HYCOM

A simulation of 40 years (CLIM) forced by climatological atmospheric fields is performed in order to test the ability of the 1/3º Atlantic configuration of HYCOM to reproduce MOW characteristics. The mechanical spin-up is achieved after 20 years.

The temperature and salinity at the Gibraltar sill, calculated by the MSBC and averaged over years 35 to 40, are 10.3°C and 38.14psu, respectively. This water then mixes with NACW whose temperature and salinity are 11.1ºC and 35.7psu, respectively. The product water introduced in HYCOM has a temperature of 10.9°C and salinity of 36.2psu, in agreement with observations (Table 1). The total MSBC transport of MOW in the Atlantic, when the modeled transport at Gibraltar of 0.8Sv, is approximately 4Sv, a slight overestimate of the observed value. The general shape of the tongue in the Atlantic Ocean is well reproduced in CLIM compared to GDEM3 (Figs. 4a and 4b): an outflow enters the basin in layers σ_2=36.38 kg/m^3 and σ_2=36.52 kg/m^3, surfaces that are neutrally buoyant around 1100m in the vicinity of the Gulf of Cadiz. The salty water (S>35.40psu) spreads westward until 40ºW and northward to 50ºN as in GDEM3. The vertical structure of the MOW in CLIM is also very close to GDEM3 (Figs. 4c and 4d) although the main

core of the MOW presents a greater westward and vertical extension in our experiment. Indeed, salinity greater than 36psu can be found as far as 20ºW and most of the MOW spreads in the Atlantic between 800m and 1300m. A reason for these differences can be attributed to the large transport of MOW imposed by the MSBC. Nevertheless, the main characteristics of the salty tongue are well reproduced and we consider the model suitable to investigate the sensitivity of the MOW.

4. Evaluation of the sensitivity of the MOW using the MSBC

4.1 Experimental set-up

In this portion of our study, we test the sensitivity of the MOW variability 1) to changes in the entrained water properties in HYCOM keeping $\Delta\rho_d$ constant and 2) to changes in MSW properties that change $\Delta\rho_d$.

1) In a first experiment, ENT, the impact of density-compensated variations of NACW properties on the MOW is considered. To that aim, we fix the temperature and salinity of the entrained water (T_{ent} and S_{ent}) at 11ºC and 35.6 psu, 0.1°C and 0.1 psu lower than what is obtained in CLIM, but with the same density (ρ_{ent}= 36.06) as CLIM. In this experiment, T_{gib}, S_{gib} and ρ_{gib} are free to evolve.

2) In order to test the sensitivity of the MOW to changes in the difference of density between MSW and NACW ($\Delta\rho_d$), we perform two experiments where two different ρ_{gib} are prescribed at the Gibraltar strait : one with Mediterranean water lighter than in CLIM (GIB_light) and one with water denser than in CLIM (GIB_dense). In CLIM, ρ_{gib} equals 38.11. In GIB_light, the temperature and salinity at the sill (T_{gib} and S_{gib}) are fixed to the observations: 13ºC and 38.4psu (ρ_{gib} = 37.67) (Baringer and Price,

1997). In GIB_dense, the MSW properties are set to 10ºC and 38.6psu (ρ_{gib} = 38.52). In these two experiments, ρ_{ent} is free to evolve and is provided by HYCOM. However, ρ_{ent} does not change much over the 40-year time period and a change in ρ_{gib} is representative of a change in $\Delta\rho_d$.

Each experiment starts from year 20 of CLIM and is integrated for an additional 20 years. All results presented in this section are averaged over the last 5 years of the simulations. The results of each experiment are summarized Table 1.

4.2 Evaluation of the entrainment

As explained in section 2.2, the first step of the MSBC consists in the calculation of water properties at Gibraltar (T_{gib}. S_{gib}, ρ_{gib} and Tr_{gib}). The second step is to determine the entrainment parameter φ. To that aim, the MSBC calculates the density difference ($\Delta\rho_d$) between the NACW (taken at 625m in HYCOM) and MSW, and the entrainment parameter φ, taking into account the geometry of the outflow region (Price and Baringer 1994). Figure 5 shows the evolution of these two parameters ($\Delta\rho_d$ and φ) for each simulation. By definition, ρ_{gib}(GIB_dense)> ρ_{gib}(CLIM) > ρ_{gib}(GIB_light). Consequently, $\Delta\rho_d$(CLIM) is greater than $\Delta\rho_d$(GIB_light) leading to a smaller entrainment parameter of 0.73 in GIB_light than in CLIM (0.79). Analogously, $\Delta\rho_d$(CLIM) is smaller than $\Delta\rho_d$(GIB_dense) leading to a much larger entrainment parameter of 0.83 in GIB_dense (Figure 5). ENT presents a $\Delta\rho_d$ and an entrainment parameter close to CLIM. All experiments slightly overestimate the observed value of the entrainment parameter (~0.7, Baringer and Price, 1997). As will be shown later in section 4.4.2, the relatively strong MSBC transport of MOW observed in all experiments

can be explained by these overestimates. With similar entrainment parameters, CLIM and ENT (Figure 5c) show similar outflow transports (~4Sv). With the largest entrainment parameters, GIB_dense has the highest transport with 4.7Sv, whereas GIB_light has the lowest with 3.5Sv.

4.3 The outflow properties

The final step of the MSBC is the calculation of the outflow properties. In ENT, we prescribe the entrained NACW 0.1psu fresher and 0.1ºC colder than in CLIM. With an entrainment parameter of 0.8, the calculation of the MSBC outflow properties in ENT (using Eqs. (1), (2) and (3) from section 2.2) yields an outflow salinity that is 0.08 psu lower than in CLIM. Indeed, with $\varphi = 0.8$, the MOW is formed by 80% of NACW and 20% of MSW. This result shows that the impact of a density-compensated change in NACW properties has more impact on the MOW properties than a change in MSW properties for entrainment parameters greater than 0.5, as expected from Eq. 3 and in agreement with the results of Baringer and Price (1997) and Xu et al. (2007).

We now analyze the results of the "non density-compensated" experiments, GIB_dense and GIB_light. The salinity and temperature at Gibraltar have been fixed to 38.6psu and 10ºC in GIB_dense. With an entrained water salinity and temperature of 35.71psu and 10.9ºC, the estimated outflow salinity and temperature are 36.19psu and 10.8ºC, respectively. However, in GIB_light where Gibraltar water salinity and temperature have been fixed to 38.4psu and 13ºC, we obtain an outflow salinity and temperature of 36.36psu and 11.8ºC. So despite a higher salinity at Gibraltar (+0.2psu), the GIB_dense outflow salinity is 0.2psu fresher than in GIB_light. This result can be

explained by the strength of the entrainment. The entrainment parameter is lower in GIB_light than in GIB_dense (0.73 compared with 0.83), meaning that less "mixing" with the NACW occurs, leading to a stronger signal of the MSW in GIB_light. If the entrainment parameter of GIB_light had been as high as the entrainment parameter of GIB_dense, the outflow salinity of GIB_light would be 36.16psu. The variation in entrainment parameter is therefore an important factor that determines the outflow property variability.

Thus, we conclude that for the parameter range explored in this study most of the MOW variability is driven by the NACW variability. However, changes in the density of NACW and/or MSW also have an important impact on the variability by changing the entrainment parameter. The relative impact of these factors is evident from an inspection of Figure 3 where it is shown that relatively small changes in the density difference create large changes in the entrainment. In these experiments, the relative change in the entrainment is greater than 10%, whereas changes in the salinity differences are less than 2%. Thus, as evident from Eq. 3, changes in the entrainment will have a greater impact on the salinity of the outflow waters. We now look at the evolution in the Atlantic Ocean of the water mass properties calculated by the MSBC for each experiment.

4.4 Water mass evolution in the Atlantic Ocean

4.4.1 General shape of the tongue

The horizontal shape and extent of the tongue remain reasonable throughout the integration of each experiment when compared to the climatology GDEM3 (Figure 7). The position of the maximum salinity core (S>36psu) is closer to the observations in

ENT than in the other experiments where it extends further westward. However, if we consider the total spreading area, we can see that CLIM and ENT are similar to GDEM3, while the spreading areas of GIB_light and GIB_dense are more confined and more extended, respectively. Specifically, if we compare the western edge of the tongue (using the isohaline 35.4psu as a boundary), we can see that GIB_light's Mediterranean tongue reaches 30ºW, GIB_dense's tongue reaches to 50ºW and GDEM3's extends to 35ºW. These results can be related to the MOW transport strength as calculated by the MSBC for each experiment. The stronger the transport, the larger the tongue's extent. GIB_dense has the strongest transport (~4.7Sv) while GIB_light has the lowest (~3.5Sv).

We now focus on the vertical shape of the salt tongue on a section at 36ºN (Figure 8). The depth of the main core differs from one experiment to another as shown in Figure 9. As a reminder, the MOW injected into the Atlantic is distributed between two selected isopycnic layers with different temperatures in such a way that the average temperature of the injected flow in both layers equals the temperature of the outflow calculated by the MSBC (See Appendix for details). Thus, GIB_light and ENT, with warmer outflows, are mainly distributed along layer 14 (σ_2=36.38) whereas GIB_dense, with the coldest outflow temperature, is mainly distributed in layer 15 (σ_2=36.52) at a lower depth. We also notice that the vertical extension of the flow differs between experiments. This vertical spreading depends on the MSBC transport of MOW, as was the case for horizontal spreading. CLIM has an outflow transport of 4Sv, with a vertical extension between 800m and 1500m. GIB_light has a transport of 3.5Sv and spreads into the Atlantic Ocean between 950m and 1100m. GIB_dense has the largest transport (4.8Sv; see Table 1) with a vertical extension of nearly 800m, between 800m and 1600m.

4.4.2 Salinity evolution

In this section, we analyze the evolution of the outflow properties in layers 14 and 15 in a box extending from 33ºN to 42ºN, and from 10ºW to 20ºW in the Atlantic Ocean (Figure 8). The evolution of the maximum salinity (Figure 10a) is comparable to the evolution of the salinity calculated by the MSBC (Figure 6f), with the highest salinity for GIB_light and the lowest for ENT. Analyzing the evolution of the spatially averaged salinity in the same box, however, yields different results (Figure 10b). While ENT still has the lowest salinity, GIB_light salinity is 0.05 psu fresher than CLIM and GIB_dense, despite the fact that its outflow salinity was 0.2 psu saltier. To understand these results, we have to take into account the salt flux $S_{out} \cdot Tr_{out}$ (in Sv psu) imported into the box (Figure 10c). GIB_dense produces the highest salt flux with 172 Sv psu, followed by CLIM and ENT with 145 and 150 Sv psu, respectively. Finally, GIB_light produces the lowest salt flux with 125 Sv psu, despite having the highest S_{out}. Comparing Figures 10c and 5c shows that the strength of these salt fluxes is induced by the MSBC transport Tr_{out} rather than the salinity S_{out}. However, since the MSBC transport Tr_{out} does not vary between CLIM and ENT, the decrease of the average salinity in the box between these two simulations is due to the decrease of S_{out}. In GIB_light, the weakness of the salt flux and, more specifically, the weakness of the transport do not allow the Mediterranean tongue to be maintained at the same salinity as in CLIM. As seen in section 4.4.1, the transport sets the amount of salt imported into the box, but also plays a role in the spatial distribution of the MOW. Figure 10d shows the ratio of the volume of water mass whose salinity exceeds 35.85psu (lowest average salinity calculated in the box, see Figure 10b)

with respect to the total volume of water in the box for each experiment. As expected from the strength of the salt flux, GIB_light ratio is small (0.30) compared with GIB_dense or CLIM ratio (0.85 and 0.70, respectively). This result shows that GIB_light Mediterranean tongue is confined to the box while GIB_dense and CLIM tongues spread more widely, giving them a potentially greater impact on the Atlantic Ocean properties and circulation. One can therefore state that, in order fully to understand the variability of the MOW in the Atlantic Ocean, the variability of the salt/heat flux of the outflow as well as the T/S properties of the outflow need to be taken into account.

5. Summary and discussion

In this study, we used the Marginal Sea Boundary Condition (MSBC) to study mechanism(s) responsible for MOW variability. To that aim, we used different sensitivity experiments to evaluate the impact of different source waters and entrained waters on the outflow properties in the Atlantic Ocean.

The analysis of the water mass transformation in the MSBC shows that the density gradient ($\Delta\rho_d$) between the Mediterranean Sea water (MSW) and the entrained water (NACW) is the dominant factor in the Mediterranean outflow process. Its value determines the entrainment parameter φ that has been evaluated between 0.73 and 0.83 in our experiments, in agreement with the observations. As a direct consequence, the variability of the MOW is more sensitive to the entrained water variability in agreement with Price and Baringer (1994) and Baringer and Price (1997). However, we also show that the entrainment parameter determines the total outflow transport and therefore the

importance of the resulting MOW salt/heat flux. The mechanism driving the outflow variability can be summarized as:

- If ρ_{ent} increases and/or if ρ_{gib} decreases, $\Delta\rho_d$ decreases leading to a lower entrainment rate φ. This leads to a decrease of the outflow transport and to a stronger influence of the Gibraltar waters at the expenses of the NACW.
- If ρ_{ent} decreases and/or if ρ_{gib} increases, $\Delta\rho_d$ increases leading to a higher entrainment rate φ. This leads to an increase of the outflow transport and to a stronger influence of the NACW at the expense of the Gibraltar waters.

In the Atlantic Ocean, we show that the evolution of the Mediterranean tongue depends not only on the T/S properties of the waters flowing out of the Gulf of Cadiz, but also on the strength of the outflow transport. Furthermore, the transport determines the importance of the spreading area and therefore the ability of the MOW to influence the Atlantic Ocean properties and circulation.

The variations of properties at Gibraltar that lead to such transport changes have been chosen purposely large compared with the observed interannual variability of these waters. Even with these large variations, the shape and water properties of the outflow tongue remain relatively stable. We therefore expect that realistic variations of the outflow transport (as in ENT compared to CLIM) will have weaker impact on the MOW variability than actual property variations of the NACW.

Following these results, the impact of changes like Eastern Mediterranean Transient on the MOW (Lascaratos et al., 1999), i.e. an increase of the density and salinity of the Gibraltar water (Millot et al., 2006), would increase $\Delta\rho_d$ and therefore the entrainment. A possible consequence of this transient on the MOW would be an

increased transport and a slightly extended tongue, but not necessarily an increase of its salinity. On a longer time scale, several scenarios of climate change have suggested that the density of the water at Gibraltar will decrease despite an increase of the salinity (Thorpe and Bigg, 2000; Somot et al., 2006). As a marginal sea, the Mediterranean Sea properties should vary faster than the open-ocean properties. Consequently, the density difference $\Delta\rho_d$ would decrease as well as the total transport of MOW, leading to a saltier but less extended tongue.

The results of this study strongly depend on the fact that the Mediterranean outflow mechanism is density-driven. This assumption has been made in most of the parameterizations of outflow including the MSBC (Turner, 1986; Price and Yang, 1998; Hallberg, 2000; Xu et al. 2006) and is based on the experimental results of Ellison and Turner (1969). We thus consider our results robust. A follow-up study will be to evaluate the impact of interannual atmospheric variability, the impact of realistic variations of the MSW properties on the MOW variability, and the role of the Meddies in the spatial expansion of MOW properties using a 1/12º configuration of the Atlantic Ocean.

Acknowledgments.

The authors want to thank Zulema Garraffo for her help in this work. This research was supported by the National Science Fondation through grant OCE-0630229. Simulations were performed at the National Center of Atmospheric Research (NCAR), Boulder, Colorado.

APPENDIX: Implementation of the MSBC in HYCOM

The first step in implementing the Price-Yang MSBC is to define the Gulf of Cadiz boundary zone at the initialization stage of each model run. The meridional boundary of this zone must be located sufficiently far to the west of the Straits of Gibraltar so that water depths exceed 1500m to permit the unimpeded injection of overflow water. The meridional boundary is therefore chosen as the first column of grid points west of the Straits where a maximum depth of 1500 m is encountered at two or more grid points within this column. This column is defined by index i_1. All grid points in and to the east of this column within the Gulf of Cadiz are then considered to be part of the boundary zone. The latitude range over which water is exchanged between the interior Atlantic and the boundary zone consists of all grid points in this column beginning with the first point located south of the latitude of the Straits and extending northward to the Iberian coast. These rows are defined by indices j_1 to j_2. The required input variables for the MSBC boundary model, T_{atl}, S_{atl}, T_{ent}, and S_{ent} (Figure 2) are all obtained from the first column of grid points to the west of the boundary longitude (index i_1-1). The MSBC subroutine always sets current velocity to zero at all u and v grid points within the boundary zone. It also initially resets the temperature, salinity, and layer thicknesses at all p grid points within the boundary zone to their climatological values with the exception of the model layers that receive the injected MOW.

The primary difficulty associated with injecting Mediterranean overflow water is that this water must be accepted by interior isopycnic layers with discrete target densities that do not match the density of the overflow water. The simplest way to do this would be to identify the model layer located just west of the boundary zone that spanned the MOW

injection depth calculated by MSBC, inject the MOW transport calculated by MSBC into this layer with the temperature and salinity values calculated by MSBC, and then rely on the hybrid vertical coordinate grid generator to re-establish isopycnic conditions in the layer. However, this requires the grid generator to move model interfaces large distances during each time step which induces large numerical diffusivity and produces highly uneven layer thicknesses in the MOW tongue west of the Gulf of Cadiz. It was therefore necessary to inject the water in a manner that preserved the isopycnic target densities in the receiving layers.

The first step of this procedure is to identify the two isopycnic layers with target potential densities that bracket the MOW density that is calculated by the HYCOM equation of state:

$$\sigma_{out} = \sigma(T_{out}, S_{out}, p_0),$$

where p_0 is the reference pressure and potential density is calculated in sigma units.
All overflow water is accepted by these layers, denoted by indices k_1 and k_2 and separated by interfaces located at pressure depths p_{k1}, p_{k2}, and p_{k3} (Figure 11). The procedure to partition the MOW injection into the two layers is designed to the greatest extent possible insure that the mass-weighted average temperature of the injected water equals T_{out} calculated by the MSBC. Within the boundary zone, the salinity in both of the two selected layers is set to S_{out} calculated by the MSBC, and then the temperature in each layer is set to

$$T_{k1out} = \sigma^{-1}(\sigma_{k1}, S_{out}, p_0)$$
$$T_{k2out} = \sigma^{-1}(\sigma_{k2}, S_{out}, p_0)\text{'}$$

where σ^{-1} signifies the inversion of the equation of state built into HYCOM to calculate temperature from potential density and salinity, and where σ_{k1} and σ_{k2} are the isopycnic target potential densities of the two layers. The pressure depth of the intermediate interface p_{k2} within the boundary zone is then reset to

$$p_{k1} = \begin{cases} p_{out} + (0.5 - q)(p_{k2} - p_{k1}) & q \le 0.5 \\ p_{out} + (0.5 - q)(p_{k3} - p_{k2}) & q > 0.5 \end{cases},$$

where

$$q = \frac{T_{k1out} - T_{out}}{T_{k1out} - T_{k2out}},$$

and where p_{out} is the central pressure depth of the injected overflow water. Note that q must be bounded between 0 and 1 because these limits can be exceeded due to the nonlinear equation of state since the two layers were selected based on their target potential densities and not temperature. The interface pressure depths above and below the two layers are then given by

$$\begin{aligned} p_{k1} &= p_{k2} + p_{k1} - p_{k2} \\ p_{k3} &= p_{k2} + p_{k3} - p_{k2} \end{aligned}.$$

All other interfaces above and below these three within the boundary zone are set to their climatological mean pressure depths except to maintain a minimum thickness of 5 m.

With layer thicknesses and water properties set at all of the grid points within the boundary zone, MOW injection into the interior Atlantic is accomplished by partitioning the total zonal transport U_{out} provided by MSBC is apportioned among the two accepting layers as

$$\begin{aligned} Tr_{k1} &= (1-q)Tr_{out} \\ Tr_{k2} &= qTr_{out} \end{aligned},$$

It is implemented by controlling the zonal velocity at the column of u grid points located immediately west of column i_1 of the pressure grid points that represent the offshore edge of the boundary zone. The zonal transport of the injected water in each layer is distributed over both the layer thickness and the meridional distance between grid point rows j_1 and j_2. To insure that there is no net zonal transport between the interior Atlantic and the boundary zone, the other two zonal transports at the edge of the boundary zone calculated by the MSBC (Tr_{atl} *and* Tr_{ent}) must also be accounted for. Both of these transports are distributed over the same latitude range (from j_1 to j_2) as Tr_{out}, but Tr_{atl} is distributed over the upper 140 m while Tr_{ent} is distributed over the depth range between 140 m and p_{k1}.

References

Arbic, B. K., Owens, W.B., 2001. Climatic Warming of Atlantic Intermediate Waters. J. of Clim. 14, 4091-4108.

Astraldi, M., Balopoulos, S., Candela, J., Font, J., Gacic, M., Gasparini, G.P., Manca, B., Theocharis, A., Tintore, J., 1999. The role of straits and channels in understanding the characteristics of Mediterranean circulation. Prog. in Oceanog. 44, 65-108.

Baringer, M. O., Price, J., 1997. Mixing and spreading of the Mediterranean outflow. J. of Phys. Oceanogr. 27, 1654-1677.

Bleck, R., 2002. An oceanic general circulation model framed in hybrid isopycnic-Cartesian coordinates. Ocean Modell. 37, 55-88.

Bower, A. S., Armi, L., Ambar, I., 1997. Lagrangian Observations of Meddy Formation

during A Mediterranean Undercurrent Seeding Experiment. J. of Phys. Oceanogr. 27, 2545-2575.

Bryden, H.L., Kinder, T.H., 1991. Steady two-layer exchange through the Strait of Gibraltar , Deep Sea Res. 38, Supplement 1A, S445-S464.

Candela, J., 2001. Mediterranean Water and Global Circulation. in: Siedler, G., Church, J., Gould, J. (Eds.), Ocean Circulation and Climate: Observing and Modelling the Global Ocean, International Geophysics Series vol 77, San Diego, 419-429.

Chassignet, E. P., Smith, L.T., Halliwell, G.T., Bleck, R., 2003. North Atlantic Simulations with the Hybrid Coordinate Ocean Model (HYCOM): Impact of the Vertical Coordinate Choice, Reference Pressure, and Thermobaricity. J. of Phys. Oceanogr. 33, 2504-2526.

Curry, R., Dickson, B., Yashayaev, I., 2003. A change in the freshwater balance of the Atlantic Ocean over the past four decades. Nature, 426, 826-829.

Ellison, T. H., Turner, J.S., 1959. Turbulent entrainment in stratified flows. J. of Fluid Mech. 6, 423-448.

Griffies, S. M., Böning, C., Bryan, F.O., Chassignet, E.P., Gerdes, R., Hasumi, H., Hirst, A., Tréguier, A.-M., Webb, D., 2000. Developments in ocean climate modelling. Ocean Modell. 2, 461-480.

Hallberg, R., 2000. Time integration of diapycnal diffusion Richardson number dependent mixing in isopycnal coordinate ocean models. Mon. Weather Rev. 128, 1402-1419.

Halliwell, G. R., 2004. Evaluation of vertical coordinate and vertical mixing algorithms in the HYbrid-Coordinate Ocean Model (HYCOM). Ocean Modell. 7, 285-322.

Hopkins, T. S., 1999. The thermohaline forcing of the Gibraltar exchange. J. of Mar. Sys. 20, 1-31.

Iorga, M. C., Lozier, M.S., 1999. Signatures of the Mediterranean outflowfrom a North Atlantic climatology 1. Salinity and density fields. J. of Geophys. Res. 104, 25 985-26 009.

Lacombe, H., Richez, C., 1982. The regime of the strait of Gibraltar. in: Nihoul, J.C.J. (Ed.), Hydrodynamics of Semi-Enclosed Seas, Elsevier Oceanography Series, Amsterdam, pp. 13-73.

Large, W. G., McWilliams, J.C., Doney, S.C., 1994. Oceanic vertical mixing: a review and a model with a nonlocal boundary layer parameterization. Rev. of Geophys. 32, 363-403.

Lascaratos, A., Roether, W., Nittis, K., Klein, B., 1999. Recent changes in deep water formation and spreading in the eastern Mediterranean Sea: a review. Prog. Oceanogr. 44, 5-36.

Leadbetter, S. J., Williams, R.J., McDonagh, E.L., King, B.A., 2007. A twenty year reversal in water mass trends in the subtropical North Atlantic. Geophys. Res. Lett. 34.

Levitus, S., Antonov, J.I., Boyer, T.P., Stephens, C., 2000. Warming of the world ocean. Science, 287, 2225-2229.

Lozier, M. S., Owens, W.B., Curry, R.G., 1995. The climatology of the North Atlantic. Progr. Oceanogr. 36, 1-44.

Lozier, M.S., Stewart, N. M., 2008. On the temporally varying northward penetration of Mediterranean Overflow Water and eastward penetration of Labrador Sea Water. J.

of Phys. Oceanogr. 38, 2097–2103. DOI: 10.1175/2008JPO3908.1

Mazé, J. P., Arhan, M., Mercier, H., 1997. Volume budget of the eastern boundary layer off the Iberian Peninsula. Deep Sea Res. I, 44, 1543-1574.

McCartney, M., Mauritzen, C., 2001. On the origin of the warm inflow to the Nordic Seas. Progr. Oceanogr. 51, 125-214.

Millot, C., 2006. Large warming and salinification of the Mediterranean outflow due to changes in its composition. Deep Sea Res. Part I, 53, 656–666.

National Geophysical Data Center, 1985. Worldwide gridded bathymetry DBDB5 5-min latitude/longitude grid. Data Announcement 85-MGG-01, NOAA/NGDC, Boulder, CO, 75 pp. [Available from NOAA, NGDC, 325 Broadway, E/GC3, Boulder, CO 80303.]

Papadakis, M. P., Chassignet, E.P., Hallberg, R.W., 2003. Numerical simulations of the Mediterranean Sea outflow: impact of the entrainment parameterization in an isopycnic coordinate ocean model. Ocean Modell. 5, 325-356.

Pinardi, N., Masetti, E., 2000. Variability of the large scale general circulation of the Mediterranean Sea from observations and modelling: a review. Palaeogeogr. Palaeoclimatol. Palaeoecol. 158, 153-173.

Potter, R. A., Lozier, M.S., 2004 On the warming and salinification of the Mediterranean outflow waters in the North Atlantic. Geophys. Res. Lett. 31, L01202.

Price, J. F., Yang, J., 1998. Marginal sea overflows for climate simulations, in: Chassignet, E.P., Verron, B. (Eds.), Ocean Modeling and Parameterization, Kluwer Academic Publishers, Dordrecht, pp. 155-170.

Price, J. F., O'Neill Baringer, M., 1994. Outflows and deep water production by marginal

seas. Progr. in Oceanogr. 33, 161-200.

Reid, J.L., 1979. On the contribution of the Mediterranean Sea outflow to the Norwegian-Greenland Sea. Deep Sea Res. 26A, 1199-1223.

Rhein, M., Hinrichsen, H.-H., 1993. Modification of Mediterranean Water in the Gulf of Cadiz. Deep Sea Res. Part A, 40, 267-291.

Rixen, M., Beckers, J.-M., Levitus, S., Antonov, J., Boyer, T., Maillard, C., Fichaut, M., Balopoulos, E., Iona, S., Dooley, H., Garcia, M.-J., Manca, B., Giorgetti, A., Manzella, G., Mikhailov, N., Pinardi, N., Zavatarelli, M., 2005. The Western Mediterranean Deep Water: a proxy for climate change. Geophys. Res. Lett. 32, L12608, doi:10.1029/2005GL022702.

Roemmich, D., Wunsch, C., 1984. Apparent changes in the climatic state of the deep North Atlantic Ocean. Nature, 307, 447-450.

Smith, R.D., Gent, P.R., 2004. Reference manual for the Parallel Ocean Program (POP),ocean component of the Community Climate System Model (CCSM2.0 and 3.0). Los Alamos National Laboratory Technical Report, LA-UR-02-2484, <http://www.ccsm.ucar.edu/models/ccsm3.0/pop>.

Somot, S., Sevault, F., Déqué, M., 2006. Transient climate change scenario simulation of the Mediterranean Sea for the twenty-first century using a high-resolution ocean circulation model. Clim. Dyn. 27, 851-879, doi:10.1007/s00382-006-0167-z.

Teague, W. J., Carron, M.J., Hogan, P.J., 1990. A comparison between the Generalized Digital Environmental Model and Levitus climatologies. J. of Geophys. Res. 95, 7167-7183.

Thorpe, R.B., Bigg, G.R., 2000. Modelling the sensitivity of the Mediterranean Outflow

to anthropogenically forced climate change. Clim. Dyn. 16, 355-368.

Turner, J.S., 1986. Turbulent entrainment: the development of the entrainment assumption, and its application to geophysical flows. J. of Fluid Mech. 173, 431-471.

Wu, W., Danabasoglu, G., Large, W.G., 2007. On the effect of parameterized Mediterranean overflow on North Atlantic ocean circulation and climate. Ocean Modell., 19, 31-52.

Xu, X., Chang, Y., Peters, H., Özgökmen, T.M., Chassignet, E.P., 2006. Parameterization of gravity current entrainment for ocean circulation models using a high-order 3D nonhydrostatic spectral element model. Ocean Modell. 14, 19-44.

Xu, X., Chassignet, E.P., Price, P.F., Özgökmen, T.M., Peters, H., 2007. A regional modeling study of the entraining Mediterranean outflow. J. of Geophys. Res. 112, C12005, doi:10.1029/2007JC004145.

Zenk, W., 1975. On the Mediterranean outflow west of Gibraltar. Meteor Forschungsergeb, 16, 23-24.

Zenk, W., Armi, L., 1990. The complex spreading pattern of the Mediterranean Water off the Portuguese continental slope. Deep Sea Res. 37, 1805-1823.

Tables

Experiments	T_{gib}, S_{gib} Gibraltar	Tr_{gib} Gibraltar	T_{ent}, S_{ent} Entrained	T_{out}, S_{out} Outflow	Tr_{out} Outflow
Observations	13ºC 38.4psu	0.7Sv-1.2Sv	11.4ºC-12.5ºC 35.6psu-35.7psu	11ºC-36.2psu	2.1Sv-4.8Sv
CLIM	10.3ºC (0.07) 38.14psu (0.02)	0.83 Sv (0.00)	11.1ºC (0.07) 35.7psu (0.02)	10.9ºC (0.07) 36.2psu (0.02)	4.0Sv (0.02)
GIB_light	**13ºC** **38.4psu**	0.87 Sv (0.00)	11.4ºC (0.09) 35.67psu (0.02)	11.8ºC (0.07) 36.36psu (0.01)	3.5 Sv (0.03)
GIB_dense	**10ºC** **38.6psu**	0.79 Sv (0.00)	10.9ºC (0.02) 35.69psu (0.01)	10.7ºC (0.02) 36.18psu (0.00)	4.8 Sv (0.05)
ENT	10.4ºC (0.16) 38.15psu (0.04)	0.83 Sv (0.00)	**11ºC** **35.6psu**	10.9ºC (0.03) 36.12psu (0.01)	4.1 Sv (0.03)

Table 1: Summary of the results averaged over years 35 to 40 of the MSBC for each experiment and observations. Values in bold type are constant during the experiment. Values in parentheses are standard deviations.

List of Figures

Figure 3: Entrainment parameter (φ) in function of $\Delta\rho_d$ (kg/m^3) for velocities at the Gibraltar strait ranged between 0.125m/s and 2.0m/s with an increment of 0.075m/s. Black lines highlight the evolution of φ for two velocities corresponding to transports at Gibraltar of 0.7Sv and 1.2Sv respectively (see Table 1).

Figure 4: Salinity averaged on layers 14 and 15 (σ_2=36.38 and σ_2=36.52, bounded by the white lines) for a) GDEM3 and b) CLIM (averaged over years 35 to 40). Vertical sections of salinity at 36ºN for c) GDEM3 and d) CLIM.

Figure 5: a) Density difference $\Delta\rho_d$ (kg/m^3) between MSW (ρ_{gib}) and NACW (ρ_{ent}), b) entrainment parameter φ for each experiment and c) MSBC transports of the Mediterranean Outflow in Sv (1Sv=10^6 kg/m^3). CLIM is in black, GIB_light in dotted-dashed black, GIB_dense in dotted gray, ENT in dashed gray.

Figure 6: Evolution of the temperature a) at Gibraltar, b) of the entrained water and c) of the Mediterranean outflow water. Evolution of the salinity d) at Gibraltar, e) of the entrained water and f) of the Mediterranean outflow water. CLIM is in black, GIB_light in dotted-dashed black, GIB_dense in dotted gray, ENT in dashed gray. The vertical dashed line indicates the end of the 20-year spin-up.

Figure 7: Salinity averaged over the sigma layers 36.18 and 36.52 for a) GDEM3, b) CLIM, c) ENT, d) GIB_dense, and e) GIB_light.

Figure 8: Location of box used for Figure 10 on salinity at 1100m (contour). The dashed line indicates the location of the section used for Figure 9.

Figure 9: Vertical section at 36ºN in the Atlantic of salinity year 40 for a) GDEM3 (climatology), b) CLIM, c) ENT, d) GIB_dense and e) GIB_light.

Figure 10: Evolution of a) the maximum of salinity of each experiment, b) the mean salinity, c) the transport of salt from the MSBC in HYCOM and, d) the volume of water mass with a salinity S>35.85psu with respect to the total volume of the box defined Figure 7. CLIM is in black, GIB_light in dotted-dashed black, GIB_dense in dotted gray, ENT is in dashed gray. The vertical dashed line indicates the end of the 20-year spin-up.

Figure 11: Schematic diagram illustrating the two layers chosen to accept the MOW injected from the Gulf of Cadiz boundary zone (right) into the interior North Atlantic (left). The solid arrows illustrate the partition of the MOW transport between the two layers while the dashed line shows the central pressure depth of the injected water calculated by the MSBC.

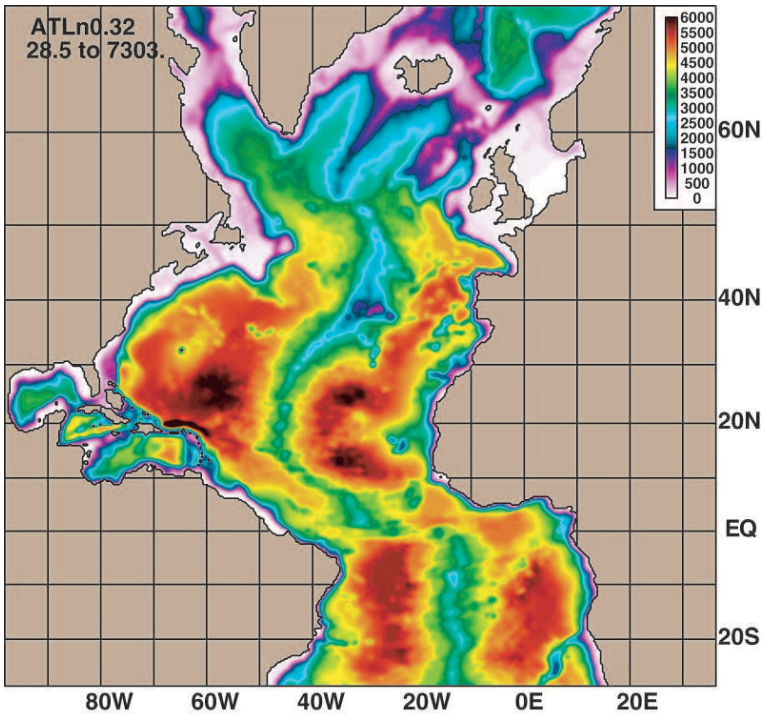

Figure 1: Bathymetry (m) of the HYCOM Atlantic Ocean configuration.

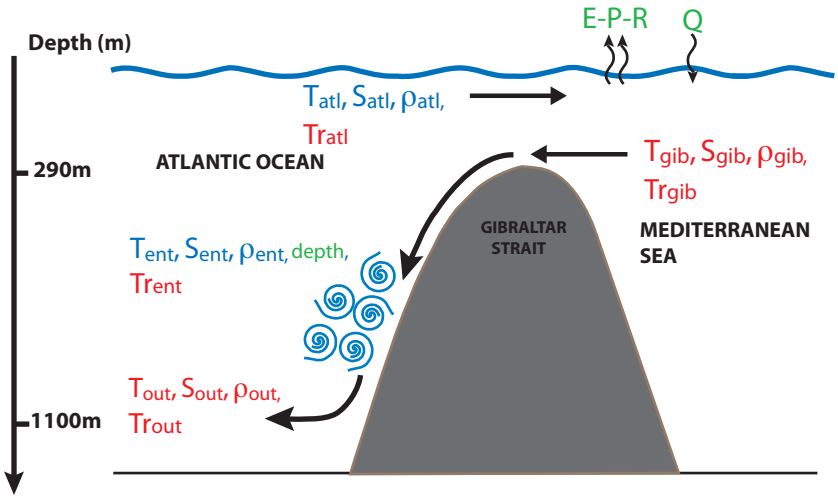

Figure 2: Schematic of the exchange at the Gibraltar strait. S_{atl} corresponds to Atlantic waters, S_{gib} corresponds to Mediterranean Sea Water at Gibraltar (source water), S_{ent} corresponds to NACW entrained water and finally S_{out} corresponds to Outflow water. Variables in green are prescribed, variables in blue are given by HYCOM and red variables are calculated by the MSBC.

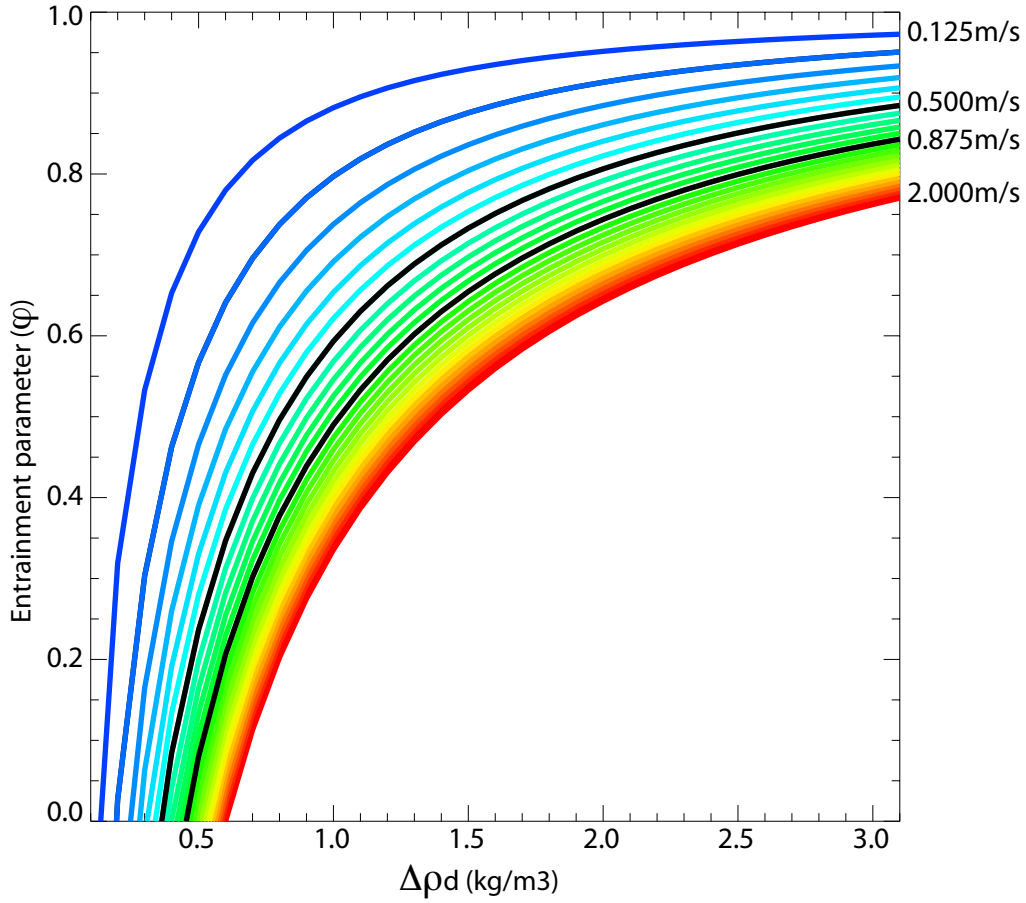

Figure 3: Entrainment parameter (φ) in function of $\Delta\rho_d$ (kg/m3) for velocities at the Gibraltar strait ranged between 0.125m/s and 2 m/s with an increment of 0.075m/s. Black lines highlight the evolution of φ for two velocities corresponding to transports at Gibraltar of 0.7Sv and1.2Sv respectively (see Table 1).

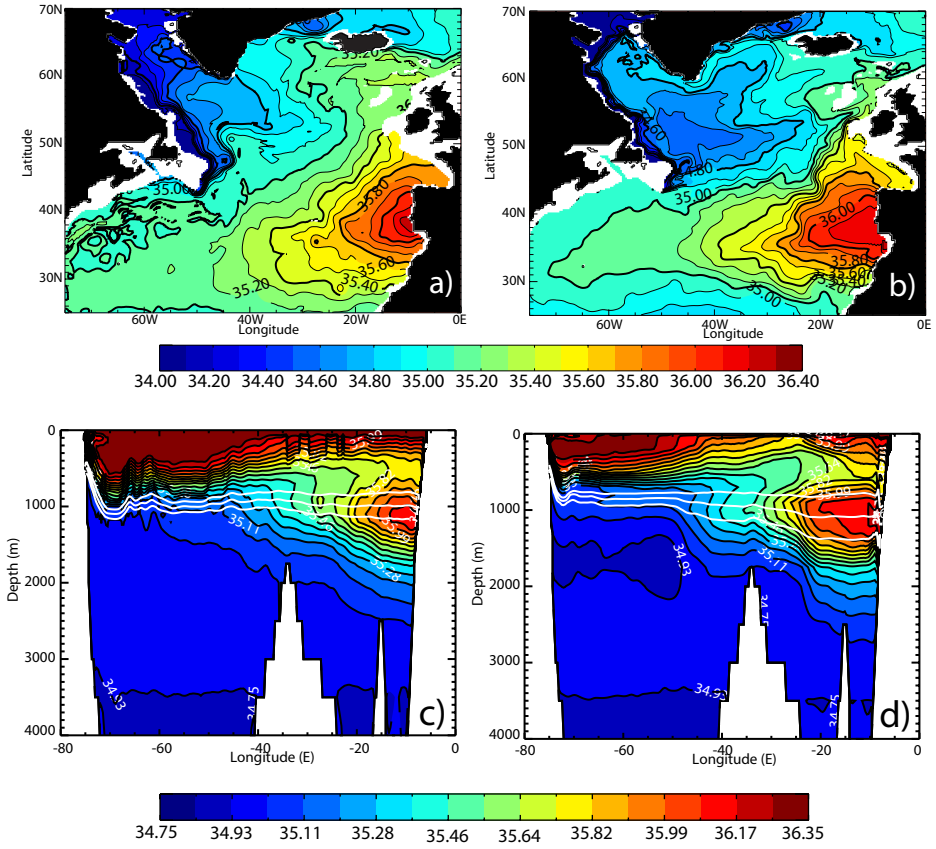

Figure 4: Salinity averaged on layer 14 and 15 ($\sigma_2 = 36.38$ and $\sigma_2 = 36.52$, bound by the white lines) for a) GDEM3 and b) CLIM (averaged over year 35 to 40). Vertical sections of salinity at 36N for c) GDEM3 and d) CLIM.

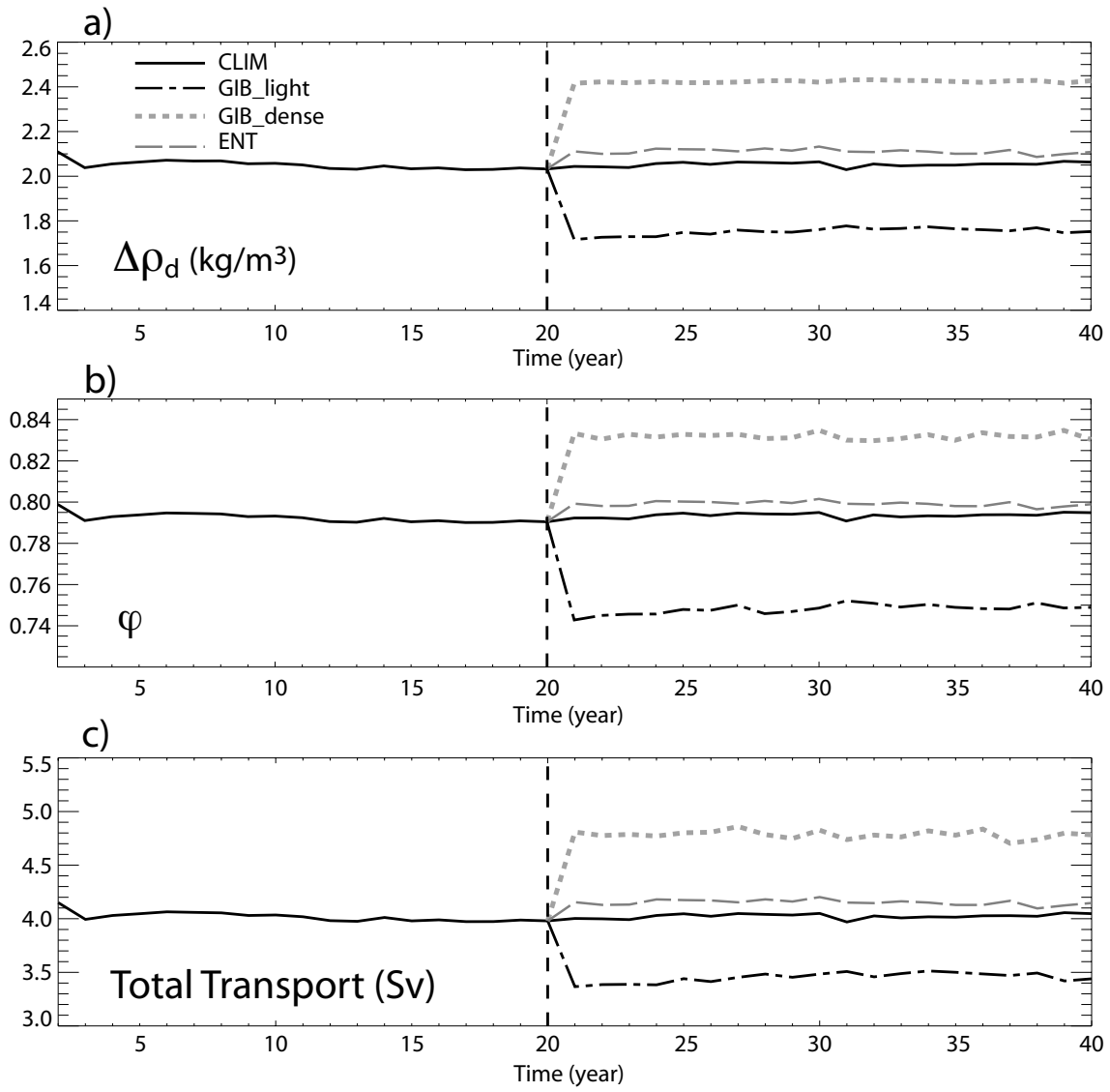

Figure 5: a) Density difference $\Delta\rho_d$ (kg/m3) between MSW and NACW, b) entrainment parameter φ for each experiment and c) transport of the Mediterranean Outflow in Sv ($1Sv = 10^6 kg/m^3$). CLIM is in black, GIB_light in dotted-dashed black, GIB_dense in dotted gray, ENT in dashed gray.

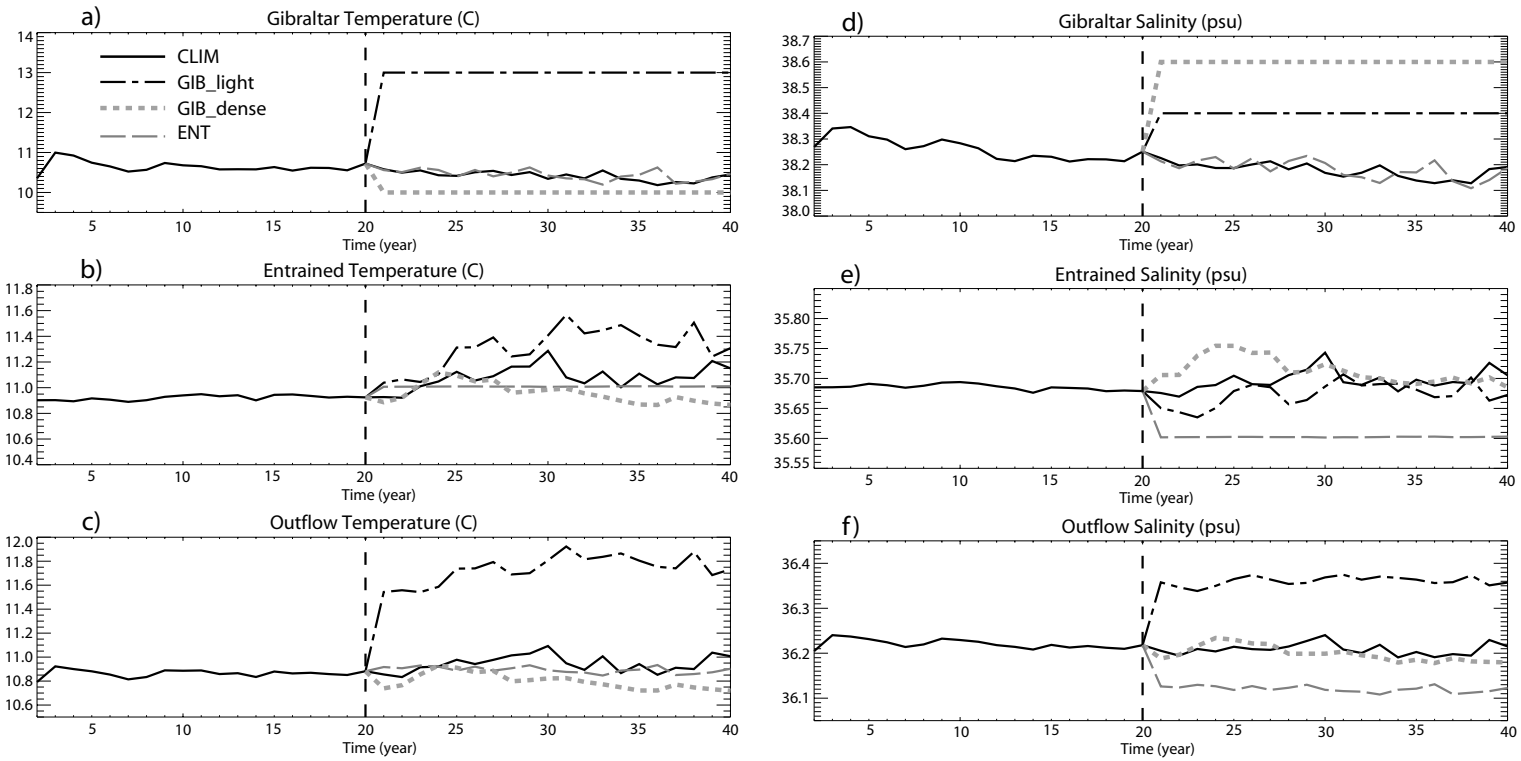

Figure 6: Evolution of the temperature a) at Gibraltar, b) of the entrained water and c) of the Mediterranean outflow water. Evolution of the salinity d) at Gibraltar, e) of the entrained water and f) of the Mediterranean outflow water. CLIM is in black, GIB_light in dotted-dashed black, GIB_dense in dotted gray, ENT in dashed gray. The vertical dashed line indicates the end of the 20-year spin-up.

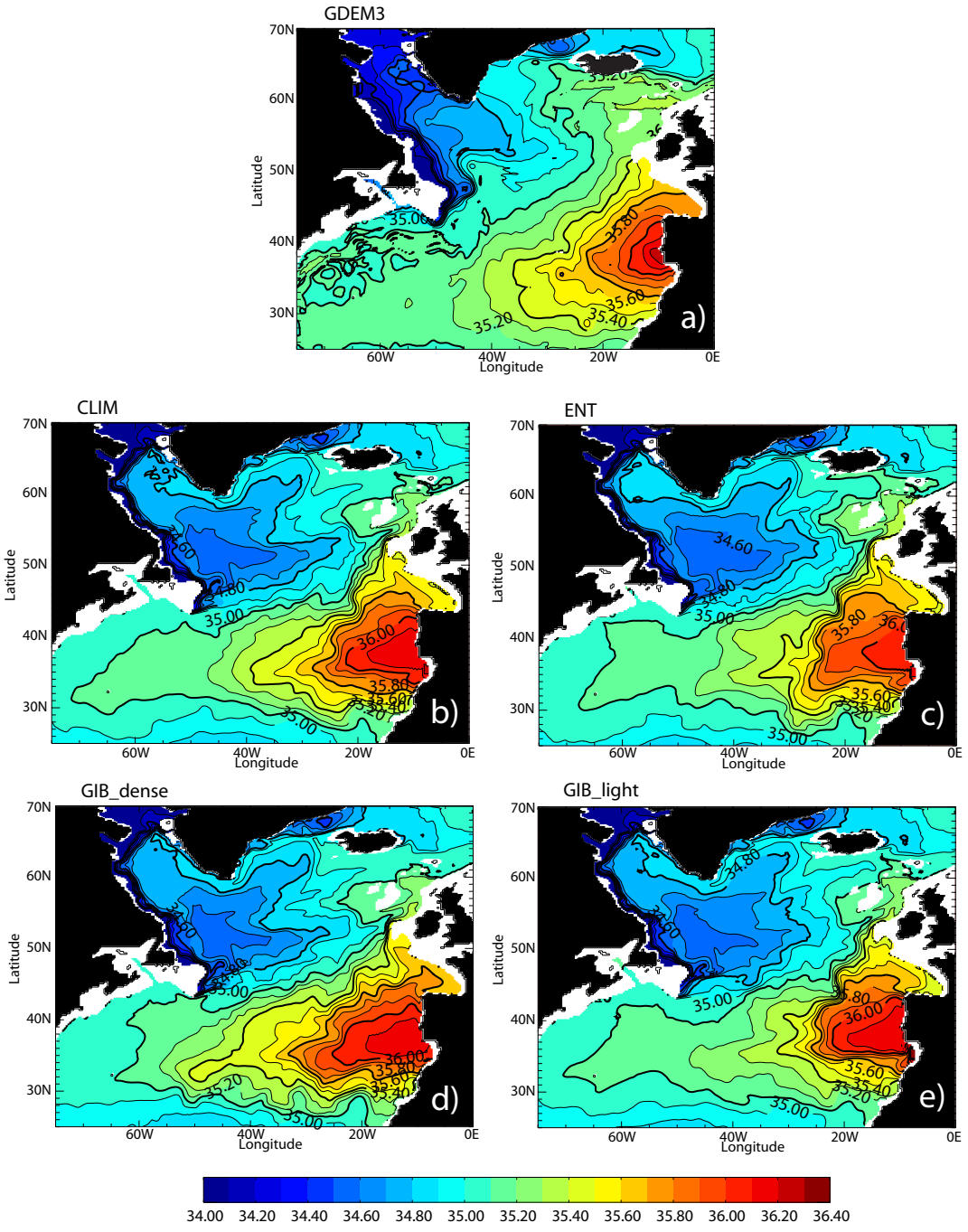

Figure 7: Salinity averaged over the sigma layer 36.18 and 36.52 for a) GDEM3, b) CLIM, c) ENT, d) GIB_dense and e) GIB_light.

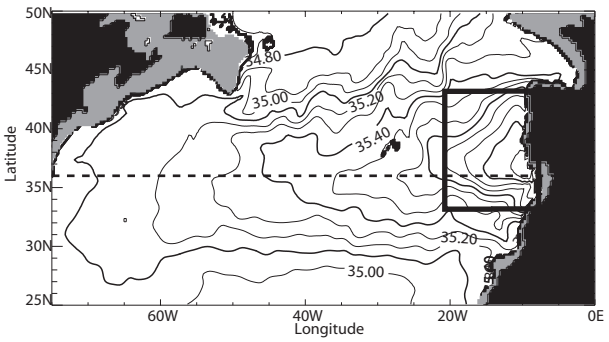

Figure 8: Location of box used for Figure 10 on salinity at 1100m (contour). The dashed line indicates the location of the section used for Figure 9.

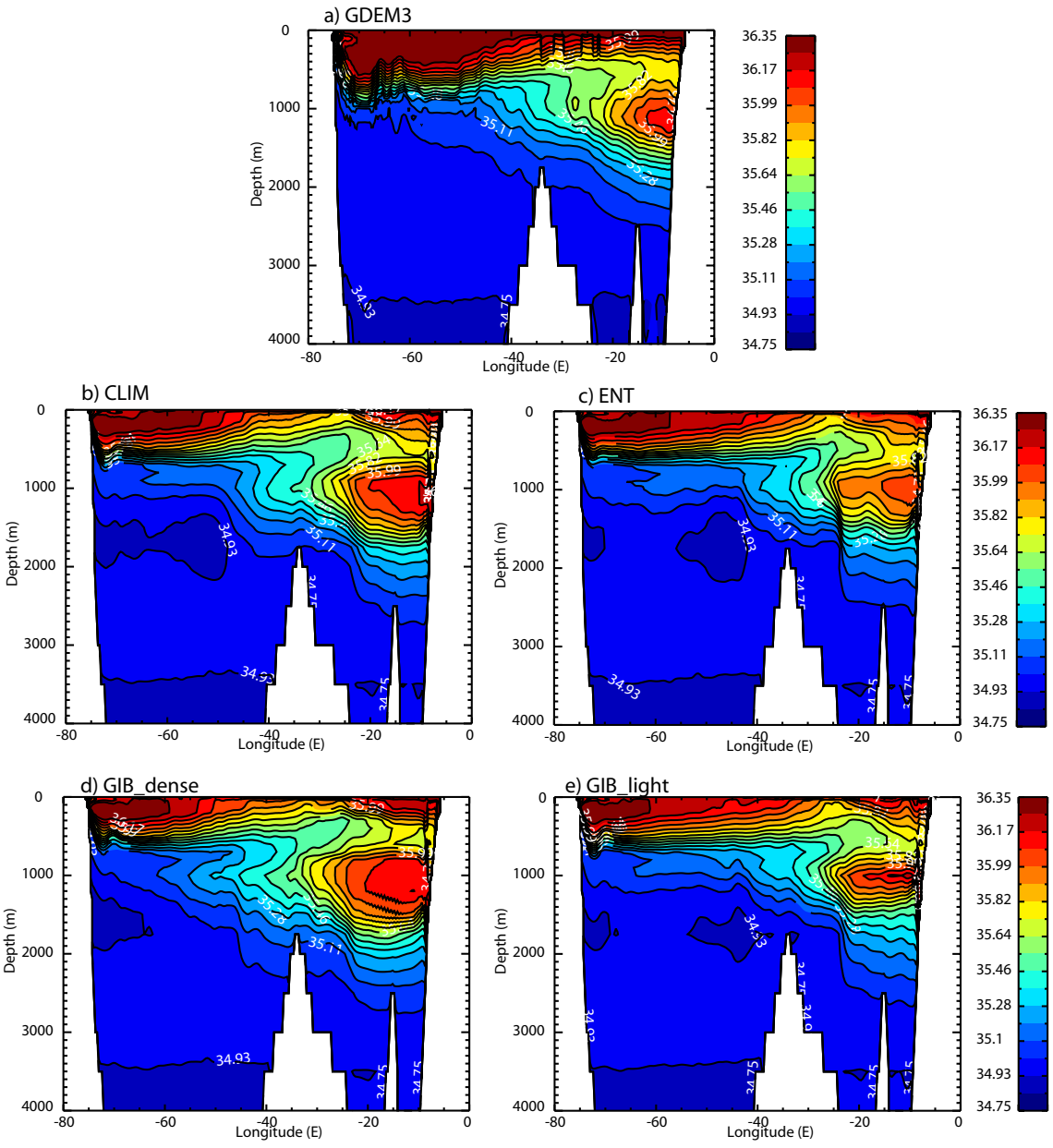

Figure 9: Vertical section at 36ºN in the Atlantic of salinity year 40 for a) GDEM3 (climatology), b) CLIM, c) ENT, d) GIB_dense and e) GIB_light.

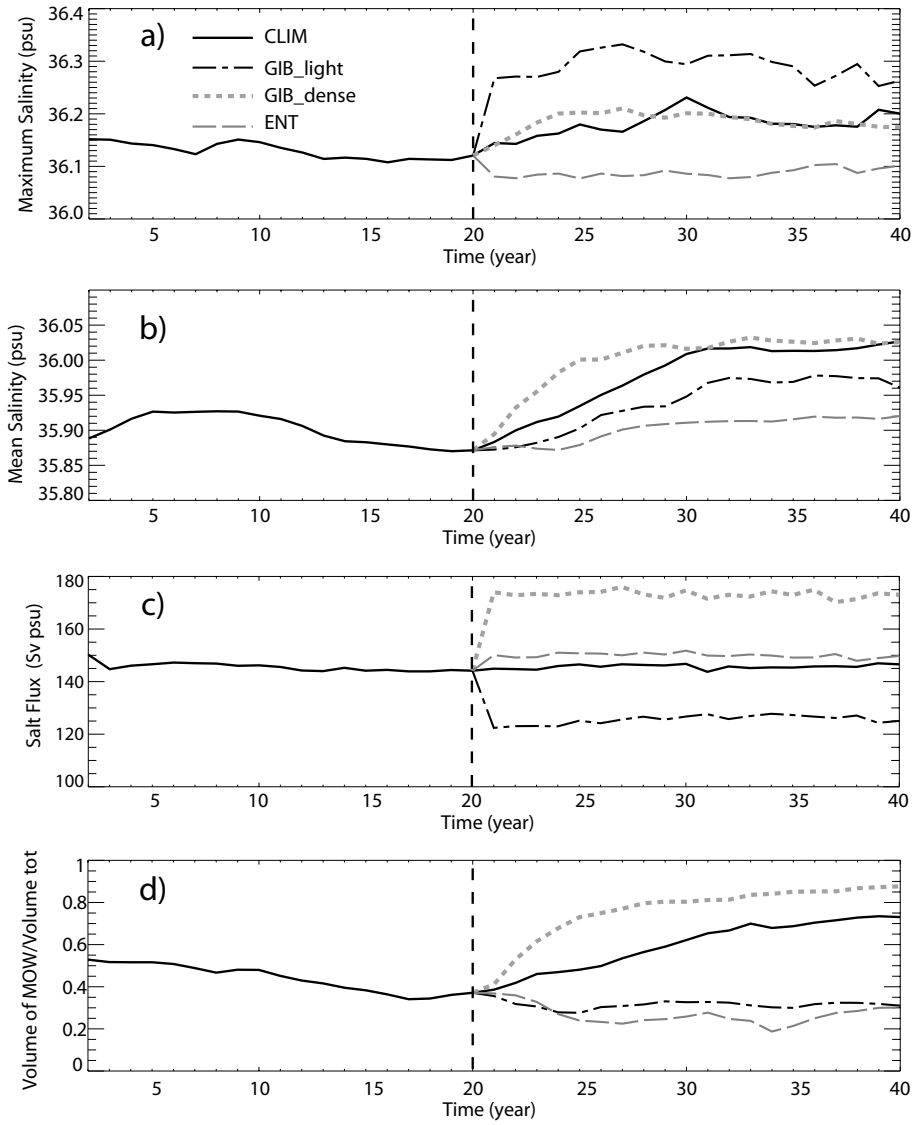

Figure 10: Evolution of a) the maximum of salinity of each experiment , b) the mean salinity, c) the transport of salt from MSBC in HYCOM and, d) the volume of water mass with a salinity $S > 35.85psu$ with respect to the total volume of the box in the box defined Figure 8. CLIM is in black, GIB_light in dotted-dashed black, GIB_dense in dotted gray, ENT is in dashed gray. The vertical dashed line indicates the end of the 20-year spin-up.

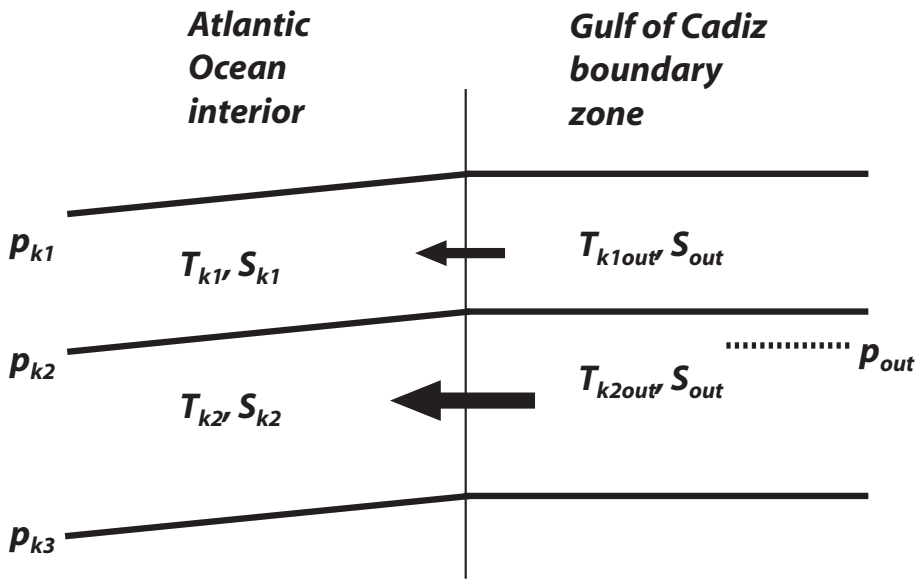

Figure 11: Schematic diagram illustrating the two layers chosen to accept the MOW injected from the Gulf of Cadiz boundary zone (right) into the interior North Atlantic (left). The solid arrows illustrate the partition of the MOW transport between the two layers while the dashed line shows the central pressure depth of the injected water calculated by the MSBC.